Selective Population and Neutron Decay of an Excited State of ^{23}O

A. Schiller,[1,*] N. Frank,[1,2,3] T. Baumann,[1] D. Bazin,[1] B. A. Brown,[1,2] J. Brown,[4] P. A. DeYoung,[5] J. E. Finck,[6] A. Gade,[1,2] J. Hinnefeld,[7] R. Howes,[8] J.-L. Lecouey,[1,†] B. Luther,[3] W. A. Peters,[1,2] H. Scheit,[1] M. Thoennessen,[1,2] and J. A. Tostevin[1,2,9]

[1]*National Superconducting Cyclotron Laboratory, Michigan State University, East Lansing, Michigan 48824, USA*
[2]*Department of Physics & Astronomy, Michigan State University, East Lansing, Michigan 48824, USA*
[3]*Department of Physics, Concordia College, Moorhead, Minnesota 56562, USA*
[4]*Department of Physics, Wabash College, Crawfordsville, Indiana 47933, USA*
[5]*Department of Physics, Hope College, Holland, Michigan 49423, USA*
[6]*Department of Physics, Central Michigan University, Mt. Pleasant, Michigan 48859, USA*
[7]*Department of Physics & Astronomy, Indiana University at South Bend, South Bend, Indiana 46634, USA*
[8]*Department of Physics, Marquette University, Milwaukee, Wisconsin 53201, USA*
[9]*School of Electronics and Physical Sciences, University of Surrey, Guildford GU2 7XH, United Kingdom*

(Received 21 December 2006; revised manuscript received 29 June 2007; published 12 September 2007)

We have observed a resonance in neutron-fragment coincidence measurements that is presumably the first excited state of ^{23}O at 2.8(1) MeV excitation energy which decays into the ground state of ^{22}O. This interpretation is consistent with theory. The reaction mechanism supports the assignment of the observed state as the $5/2^+$ hole state. This assignment and the recently observed $3/2^+$ particle state advance the understanding of ^{23}O.

DOI: 10.1103/PhysRevLett.99.112501 PACS numbers: 21.10.Pc, 25.60.Je, 27.30.+t, 29.30.Hs

Magic numbers are pillars of our understanding of nuclear structure. Nuclei with one nucleon added (removed) from a doubly magic core can be described by a (quasi-) single-particle (SP) model. The emergence of magic numbers is due to the presence of gaps in the SP spectrum around the Fermi energy. For energy gaps larger than the strength of residual interactions such as pairing or quadrupole-quadrupole forces, correlations are weak and no corresponding low-lying collectivity is observed.

Magic numbers follow harmonic-oscillator shells up to N, $Z = 20$. For heavier nuclei, the spin-orbit splitting between high-l orbitals produces N, $Z = 28$, 50, 82, and 126. The emergence of new shell gaps in light nuclei far from stability is thought to be related to the effect of the tensor force [1]. The (average) monopole contribution of this two-body interaction can be taken into account through effective SP (ESP) energies which depend on occupation numbers. The universal *sd*-shell (USD) interaction takes into account the effects of residual forces through a fit to experimental data. Using the new USD-B shell interaction to calculate the neutron ESP spectra for neutron-rich oxygen isotopes reveals large gaps for ^{22}O and ^{24}O at the Fermi energy. Therefore, both nuclei are predicted to show characteristics associated with magic nuclei [2]. This is confirmed by a high 2^+ energy in the case of ^{22}O [3] and by studies of neutron-separation energy systematics in the case of ^{24}O [4]. ^{23}O is sandwiched by these two nuclei with significant subshell gaps, and its excitation spectrum is of importance for shell-model calculations. While a recent pickup reaction populated the $3/2^+$ particle state probing the $N = 16$ gap [5], the present Letter reports on the $5/2^+$ hole state which is sensitive to the $N = 14$ gap.

We have populated the n-^{22}O continuum by $2p + 1n$ removal from a ^{26}Ne beam and reconstructed the decay-energy spectrum of excited ^{23}O in order to search for resonances corresponding to unbound states. Two-valence-proton knockout reactions are a good tool to study the nuclear structure of rare isotopes since they leave the remaining nucleons largely undisturbed [6]. In this Letter, we use the removal of three nucleons, one of them possibly an inner-shell proton, and argue that this reaction populates the n-^{22}O continuum selectively.

The experiment was performed at the National Superconducting Cyclotron Laboratory at Michigan State University. A 105 pnA primary beam of 140 MeV/A ^{40}Ar impinged on a 893 mg/cm^2 Be production target. ^{26}Ne at 86 MeV/A was produced using an achromatic 750-mg/cm^2-thick acrylic wedge degrader and either 1% or 3% momentum-acceptance slits at the dispersive focal plane as well as ± 10 mm slits at the extended focal plane of the A1900 fragment separator [7]. A purity of up to 93.2% was achieved with a ^{26}Ne beam intensity of about 7000 pps. The contaminants (mainly ^{27}Na and ^{29}Mg) were separated event-by-event in the offline analysis by their different time of flight (TOF) from the extended focal plane to a scintillator in front of the 721-mg/cm^2-thick Be reaction target. This also gives the time of beam interaction with the target t_0. Positions and angles of incoming beam particles were measured by two 15×15 cm^2 position-sensitive parallel-plate avalanche counters (PPACs) with $\sim$8 pads/cm, i.e., FWHM $\approx$ 1.3 mm. The presence of a quadrupole triplet downstream of the PPACs translates this into a position resolution of impinging ^{26}Ne particles on the reaction target within a FWHM radius of 2.4 mm.

Charged particles behind the reaction target were bent 43° by the large-gap 4 Tm sweeper magnet [8]. Two 30 × 30 cm^2 cathode-readout drift chambers (CRDCs) provided position in the dispersive (~ 4 pads/cm, FWHM ≈ 2.5 mm) and nondispersive (drift time, FWHM ≈ 3.1 mm) direction. The 1.87 m distance between the CRDCs translates this into FWHM = 2.4 mrad angle resolution. Energy loss was determined in a 65-cm-long ion chamber and a 40 × 40 cm^2, 4.5-mm-thin plastic scintillator whose pulse-height signal was corrected for position. Energy loss was used to separate reaction products with different Z [see Fig. 1(a)]. The thin scintillator also gave TOF of reaction products from the reaction target with respect to t_0. This, together with the total kinetic energy (TKE) measurement in a 15-cm-thick plastic scintillator, provided isotopic separation [see Figs. 1(b) and 1(d)].

The pulse-height signal of the thick scintillator was also corrected for position. The raw TOF was corrected for (i) position on the thin scintillator, (ii) angle and position behind the sweeper magnet, and (iii) the point of interaction on the target. The TOF corrections approximately compensate for the spread in energy of reaction products and account for differences in length of the fragment tracks and of the light paths in the thin scintillator. Because of the finite acceptance, a magnetic-rigidity range of reaction products is selected. For reaction products with equal Z, this translates into TKE $\propto 1/A$ and ToF $\propto A$ [see Fig. 1(b)]. This finite acceptance and the fact that the experiment ran in coincident mode prevented observation of ^{24}O in our setup.

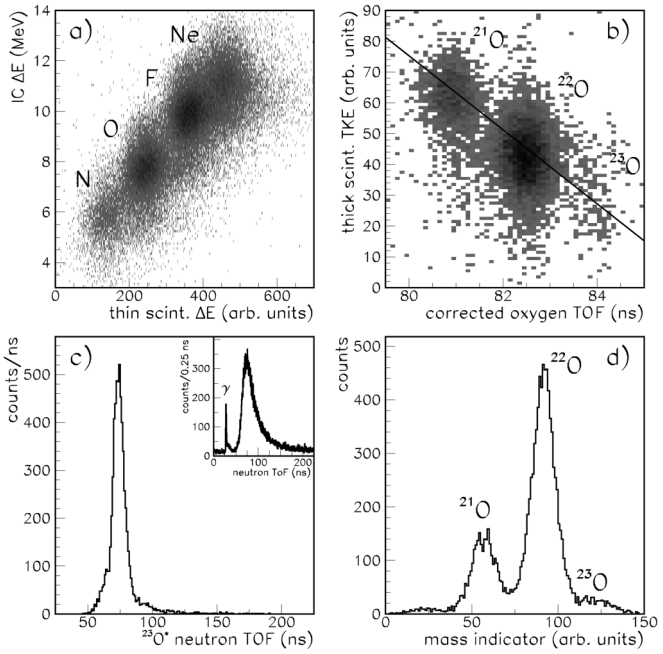

FIG. 1. (a) Energy losses in thin scintillator and ion chamber provide Z identification. (b) TKE in thick scintillator vs corrected TOF for oxygen fragments provides isotope identification. (c) Neutron TOF for decay of ^{23}O*, i.e., in coincidence with ^{22}O fragments, and using a thick target in singles mode which also produces prompt γ radiation (inset). The 1.4 ns FWHM of the γ peak translates into a neutron-energy resolution of 1.4 MeV. (d) A one-dimensional mass-indicator spectrum for oxygen fragments is obtained by projecting the data from panel (b) onto the diagonal line there.

Beam-velocity neutrons were detected in the modular neutron array (MoNA) [9] at a distance of 8.2 m from the reaction target with an intrinsic efficiency of ~70%. MoNA consists of 9 × 16 stacked 2-m-long plastic scintillator bars which are read out on both ends by photomultiplier tubes (PMT). The bars are mounted horizontally and perpendicular to the beam axis. Position along the vertical and along the beam axis is determined within the thickness of one bar (10 cm). Horizontal position and neutron TOF are determined by the time difference and the mean time, respectively, of the two PMT signals which yield resolutions of FWHM ≈ 12 cm and FWHM ≈ 0.24 ns. The TOF spectrum was calibrated by shifting the prompt γ-ray TOF peak from a thick-target MoNA singles run to 27 ns with respect to t_0 [see inset in Fig. 1(c)]. A neutron TOF spectrum (first hit after t_0 + 30 ns) in coincidence with ^{22}O fragments is given in Fig. 1(c).

The decay energy of resonances is reconstructed by the invariant mass method. The relativistic four-momentum vectors of the neutron and fragment are reconstructed at the point of breakup. For neutrons, position and TOF resolution translate into angle and energy resolution of FWHM = 19 mrad and FWHM = 3.8 MeV [10], respectively. The angle and energy of fragments in coincidence with neutrons were reconstructed behind the reaction target based on the ion-optical properties of the sweeper magnet and taking into account the position at the target in the dispersive direction available through forward tracking from the PPACs [11]. The target position in the nondispersive direction serves as a check parameter. The angle and energy resolution of the fragments behind the target are FWHM = 6.4 mrad and FWHM = 0.9 MeV/A, respectively. The average energy loss of the fragment through half of the reaction target is added to approximate the relativistic four-momentum vector of the fragment at the average breakup point.

The experiment ran for two days and produced 5700 n-^{22}O coincidences. The reconstructed decay-energy spectrum from n-^{22}O coincidences is shown in Fig. 2. This spectrum is affected by the finite acceptance for fragments and neutrons. It is biased toward the fastest neutron for events where more than one neutron hit MoNA because in the analysis, only the first hit after ~27 ns is taken into account. Later hits due to either multiple scattering of one neutron or true multiple-neutron events are ignored in the analysis [11]. The most severe of these effects, namely, the one due to acceptance cuts, has been simulated. In general, it results in a strongly decreasing detection probability and a worsening energy resolution for high decay-energy events (see Fig. 2). In the simulation, a Glauber reaction model is used. Angle straggling of the fragments in the target is taken into account, as well as detector resolutions.

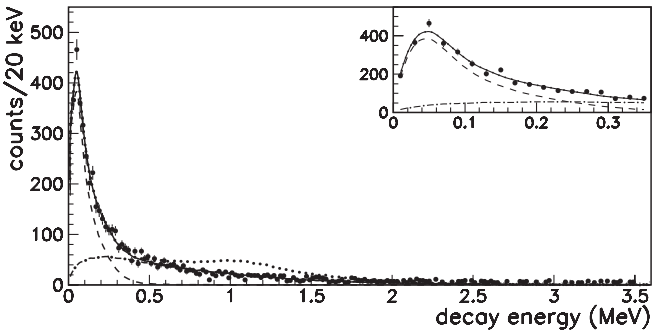

FIG. 2. Decay-energy spectra of $^{23}O^*$ (data points). The inset shows a close-up of the first 360 keV. The thick solid curve corresponds to the sum of the dashed (simulated resonant contribution) and dash-dotted (simulated thermal model) curves and agrees well with the data. Adding a strongly populated second resonance at a higher energy as observed in Ref. [5] (dotted line) is not consistent with our data. The nonobservation of the second resonance corresponds to an upper limit of its population of ~20% relative to the first resonance. The thin solid curve indicates the simulated effect of the geometric acceptance on the reconstructed decay-energy spectrum, by assuming an energy-independent decay energy.

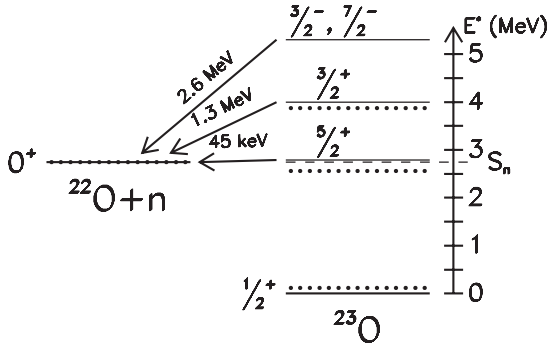

FIG. 3. Comparison of ^{23}O excitation spectrum (this work and [5]) to theory [15] (dotted lines, calculation relative to the ^{22}O ground state, using the HBUSD interaction, a version of the old USD interaction which is slightly modified for heavier isotopes). The negative-parity state in ^{23}O is outside of the USD model space. The agreement is of a similarly good quality as for the ^{22}O excitation spectrum [3], and hence supports the assumed presence of large gaps in the single-particle spectrum at the Fermi energy for $^{22,24}O$.

The n-^{22}O data in Fig. 2 are best described by a Breit-Wigner resonance contribution (dashed curve)

$$\sigma(E) \propto \frac{\Gamma}{(E - E_r)^2 + \Gamma^2/4}, \tag{1}$$

with $E_r = 45(2)$ keV and an energy-independent SP width of $\Gamma \sim 0.1$ keV plus a contribution from a beam-velocity source of Maxwellian-distributed neutrons (a thermal model) with $T \sim 0.7$ MeV (dash-dotted curve). The ratio of the contributions is 1:2. The simulated decay-energy resolution, in qualitative agreement with [12], is found to scale as FWHM $\sim 16\sqrt{E}$ and $40\sqrt{E}$ (all energies in keV), below and above $E = 1.5$ MeV decay energy, respectively. The numerical factors are dominated by neutron-angle resolution and target thickness. For the present resonance, the width due to experimental conditions (100 keV) overshadows the Wigner limit by about 3 orders of magnitude. Hence its lifetime is not determined. The thermal model has been included in the fit as a phenomenological description for what we think is mostly a low decay energy, nonresonant contribution to the spectrum. The contributions from uncorrelated and high decay-energy neutrons are small due to the low event rate and the small geometric acceptance for such events, respectively. Both contributions have been simulated by event mixing [13] and by assuming neutron decay from the high-energy excitations of ^{24}O discussed in the following paragraph. The resulting shapes do not differ substantially from the thermal model. The presence of a nonresonant background in similar experiments has also been observed by other groups [12,14].

The observation of only one resonance in the decay-energy spectrum might indicate selectivity of the reaction. The spectrum of ^{23}O from Fig. 3 has a $5/2^+$ state [a $\nu(0d_{5/2})^{-1}$ hole state with a filled $\nu(1s_{1/2})^2$ orbital] and a $3/2^+$ state [a $\nu(0d_{3/2})^1$ particle state with an empty $\nu(1s_{1/2})^0$ orbital] as observed in [5]. Equal population of these states is inconsistent with our data (see dotted line in Fig. 2). Preferred population of the $5/2^+$ state is consistent with a direct three-nucleon knockout mechanism from ^{26}Ne whose ground-state wave function [16] has large spectroscopic overlap with the ^{23}O $1/2^+$ ground state [a $\nu(1s_{1/2})^{-1}$ hole state] and the $5/2^+$ excited state, but a factor of ~10 smaller overlap with the $3/2^+$ excited state. Knockout of both valence protons will simply populate the ^{24}O ground state. However, two-proton knockout [17] from ^{26}Ne involving one core $\pi(0p)$ and one valence $\pi(0d_{5/2})$ proton populates a wide distribution of GDR-like negative-parity cross-shell excitations in ^{24}O. Such excitations should decay via negative-parity neutron-excitation admixtures of the form $\nu(0p)^{-1}\nu(0d_{3/2})^1$, $\nu(0d_{5/2})^{-1}\nu(0f1p)^1$, and $\nu(1s_{1/2})^{-1}\nu(0f1p)^1$. The first of these has large spectroscopic overlap with high-lying negative-parity excitations in ^{23}O. The other two will likely decay by neutron emission to the ^{23}O $5/2^+$ excited and $1/2^+$ ground state, respectively, and not to the $3/2^+$ excited state. The subsequent neutron decay of the $5/2^+$ state is the resonance observed in our experiment. Both proposed reaction mechanisms are consistent with our observations. Assuming uncorrelated nucleons and removal only by the stripping mechanism, calculated cross sections for $\pi(0p) + \pi(0d_{5/2})$ and $\pi(0d_{5/2})^2 + \nu(0d_{5/2})^1$ removal are $\sigma = 2.4$ and 0.12 mb, respectively.

The decay energy [45(2) keV] of the resonance can be related to excitation energy [2.79(13) MeV] by adding the neutron-separation energy $S_n = 2.74(13)$ MeV of ^{23}O [18] under the assumption that the decay populates the ground state of ^{22}O. This assumption could be wrong in two scenarios. First, if the neutron decay from the $5/2^+$ state

was to the first excited state in ^{22}O at 3.2 MeV [a $\nu(0d_{5/2})^{-1}\nu(1s_{1/2})^{-1}$ configuration], it would be by s-wave emission with a large spectroscopic overlap. However, the resonance shape of the decay-energy spectrum is inconsistent with s-wave neutron emission. Moreover, the then 3.2 MeV mismatch between theory and experiment for the $5/2^+$ state of ^{23}O would be hard to reconcile with the good agreement between theory and experiment of the ^{22}O spectrum which largely involves $\nu(0d_{5/2})^{-1}$ holes [15]. Second, a high-lying excited state (not the $5/2^+$ state) could neutron decay to excited states in ^{22}O and produce the resonance in our spectrum. However, one would then still expect to see neutron decay from the $5/2^+$ state, which is thought to be populated strongly in the reaction, as a second resonance in the spectrum.

Using new USD-B wave functions [2], the spectroscopic factor for the neutron decay of the $5/2^+$ state of ^{23}O to the ground state of ^{22}O is 0.059, which is also the reason why the state would not have been observed by Elekes *et al.* [5]. Thus, with a calculated d-wave neutron SP width of 90(10) eV (based on 45 keV decay energy), the total decay width of 5.0(6) eV is extremely small. Still, the calculated γ-decay lifetime is 4.5 ps corresponding to a partial width of only 0.15 meV.

In conclusion, observation of the $5/2^+$ hole state at 45(2) keV above S_n corresponding to an excitation energy of 2.79(13) MeV confirms the presence of a large $N = 14$ gap in neutron-rich oxygen isotopes. Together with the finding of the large $N = 16$ gap through the observation of the $3/2^+$ particle state at 4 MeV this establishes ^{23}O as a unique nucleus with two large subshell gaps consistent with the USD shell-model calculations.

We would like to thank the members of the MoNA Collaboration, G. Christian, C. Hoffman, K. L. Jones, K. W. Kemper, P. Pancella, G. Peaslee, W. Rogers, S. Tabor, and about 50 undergraduate students for their contributions to this work. We would like to thank R. A. Kryger, C. Simenel, J. R. Terry, and K. Yoneda for their valuable help during the experiment. Financial support from the National Science Foundation under Grants No. PHY-01-10253, No. PHY-03-54920, No. PHY-05-55366, No. PHY-05-55445, and No. PHY-06-06007 is gratefully acknowledged. J. E. F. and J. T. acknowledge support from the Research Excellence Fund of Michigan and from the United Kingdom Engineering and Physical Sciences Research Council (EPSRC) under Grant No. EP/D003628, respectively.

*schiller@nscl.msu.edu
†Present address: Laboratoire de Physique Corpusculaire, ENSICAEN, IN2P3, 14050 Caen, Cedex, France.

[1] T. Otsuka *et al.*, Phys. Rev. Lett. **87**, 082502 (2001); T. Otsuka, T. Suzuki, R. Fujimoto, H. Grawe, and Y. Akaishi, *ibid.* **95**, 232502 (2005); T. Otsuka, T. Matsuo, and D. Abe, *ibid.* **97**, 162501 (2006).
[2] B. A. Brown and W. A. Richter, Phys. Rev. C **72**, 057301 (2005); **74**, 034315 (2006).
[3] M. Stanoiu *et al.*, Phys. Rev. C **69**, 034312 (2004).
[4] A. Ozawa, T. Kobayashi, T. Suzuki, K. Yoshida, and I. Tanihata, Phys. Rev. Lett. **84**, 5493 (2000).
[5] Z. Elekes *et al.*, Phys. Rev. Lett. **98**, 102502 (2007).
[6] D. Bazin *et al.*, Phys. Rev. Lett. **91**, 012501 (2003); D. Warner, Nature (London) **425**, 570 (2003); J. Fridmann *et al.*, *ibid.* **435**, 922 (2005).
[7] D. J. Morrissey, B. M. Sherrill, M. Steiner, A. Stolz, and I. Wiedenhoever, Nucl. Instrum. Methods Phys. Res., Sect. B **204**, 90 (2003).
[8] M. D. Bird *et al.*, IEEE Trans. Appl. Supercond. **15**, 1252 (2005).
[9] B. Luther *et al.*, Nucl. Instrum. Methods Phys. Res., Sect. A **505**, 33 (2003); T. Baumann *et al.*, *ibid.* **543**, 517 (2005).
[10] The nominal energy resolution of FWHM = 1.6 MeV is degraded by a systematic TOF walk with deposited energy. This walk does not affect the position resolution along a bar, nor can it be corrected due to inefficiencies of the charge-signal collection. Furthermore, the effect on the decay-energy resolution is negligible, as it is determined mostly by the neutron-angle resolution and the target thickness.
[11] N. Frank, Ph.D. thesis, Michigan State University, 2006.
[12] N. Fukuda *et al.*, Phys. Rev. C **70**, 054606 (2004).
[13] F. M. Marqués *et al.*, Phys. Lett. B **476**, 219 (2000).
[14] F. Deák *et al.*, Nucl. Instrum. Methods Phys. Res., Sect. A **258**, 67 (1987); S. D. Pain *et al.*, Eur. Phys. J. A **25**, 349 (2005); Phys. Rev. Lett. **96**, 032502 (2006).
[15] A. Volya and V. Zelevinsky, Phys. Rev. Lett. **94**, 052501 (2005).
[16] J. R. Terry *et al.*, Phys. Lett. B **640**, 86 (2006).
[17] J. A. Tostevin and B. A. Brown, Phys. Rev. C **74**, 064604 (2006).
[18] G. Audi, A. H. Wapstra, and C. Thibault, Nucl. Phys. **A729**, 337 (2003).